Total Routhian surface calculations of triaxial or γ-soft properties in even-A $N=76$ isotones with $54\leqslant Z\leqslant 68$ *

YANG Qiong(杨琼)[1] WANG Hua-Lei(王华磊)[1;1)] CHAI Qing-Zhen(柴清祯)[1] LIU Min-Liang(柳敏良)[2]

[1] School of Physics and Engineering, Zhengzhou University, Zhengzhou 450001, China
[2] Institute of Modern Physics, Chinese Academy of Sciences, Lanzhou 730000, China

Abstract: Total Routhian surface (TRS) calculations for even–even $N=76$ isotones with $54\leqslant Z\leqslant 68$ have been performed in three-dimensional (β_2,γ,β_4) deformation space. Calculated results of the equilibrium deformations are presented and compared with other theoretical predictions and available experimental data. The behavior of collective angular momentum shows the neutron rotation-alignment is preferred in the lighter $N=76$ isotones, while for the heavier ones the proton alignment is favored. Moreover, multi-pair nucleon alignments and their competition (e.g., in ^{144}Er) are predicted. It is pointed out that these nuclei in the $N=76$ isotonic chain exhibit triaxiality or γ softness in high-spin states as well as ground states. Based on deformation-energy curves with respect to axial and non-axial quadrupole deformations, the shape instabilities are evaluated in detail and predicted, particularly in γ direction. Such instabilities are also supported by the odd- and even-spin level staggering of the observed γ bands, which is usually used to distinguish between γ-rigid and γ-soft asymmetry.

Key words: total Routhian surface calculation, triaxial deformation, γ-instability, rotation alignment

PACS: 21.10.Re, 21.60.Cs, 21.60.Ev **DOI:** 10.1088/1674-1137/39/9/094102

1 Introduction

The geometric shape is an essential property of a nucleus and can usually be changed by particle-hole excitation, broken-pair excitation and rotational motion. So far, it is found that atomic nuclei may exhibit a variety of shapes, such as prolate or oblate spheroids. As one way, nuclear shape can be described by the parameterization of nuclear surface, e.g. the multipole expansion with the Laplace spherical harmonics [1]. Due to the limitation in deformation multipolarity, the low-order members of the spherical harmonics expansion are expected to be important [2]. Indeed, the quest for non-axial quadrupole deformation (triaxial γ deformation) of the nucleus is still one of the major issues in nuclear structure physics.

The triaxial γ deformation will manifest itself experimentally by the wobbling mode [3], signature inversion (or splitting) [4] and chiral doublets [5]. On the theoretical side, since there are still many difficulties in understanding such phenomenon from first principles, numerous studies are mainly performed in terms of various models including the macroscopic-microscopic (MM) model [6, 7], the rigid triaxial rotor model (RTRM) [8], the triaxial projected shell model (TPSM) [9], the interacting boson model (IBM) [10, 11], the fermion dynamical symmetry model (FDSM) [12], the relativistic mean field model (RMF) [13] and the pair-truncated shell model (PTSM) [14], etc. Nevertheless, each of these can only partly explain the observed phenomena in nuclei. To obtain a better understanding of the triaxial or γ-soft properties and their mechanisms, a systematic investigation is necessary, especially for transitional mass regions.

As is known, the transitional nuclei, such as A=130–140 mass region, have γ-soft shapes and are difficult to describe by theory because their structural characteristics are more complicated than those of spherical or well-deformed regions. For instance, a lot of phenomena including prolate, oblate and triaxial collective excitation, shape coexistence and quasi-particle excitation (e.g., high-K isomer) are all identified at similar energies in experiments [15–21]. Moreover, nuclei near the neutron number $N=76$ are suggested to be more γ-rigid in this region [22]. Experimentally, high-spin structures including quasi-γ bands have been observed in the even–even $N=76$ isotones ranging from ^{130}Xe to ^{140}Gd [15]. These provide us with the necessary information for testing and predicting the triaxiality or γ softness in this

Received 16 December 2014
* Supported by National Natural Science Foundation of China (10805040, 11175217), Foundation and Advanced Technology Research Program of Henan Province(132300410125), S & T Research Key Program of Henan Province Education Department (13A140667)
1) E-mail: wanghualei@zzu.edu.cn

isotonic chain. These signatures in low-lying nuclear states have been discussed based on a rigid triaxial potential [8] and a completely γ-flat potential [23]. These two potentials would, however, not produce such different nuclear spectra as expected [24]. The IBM, in which the Hamiltonian has exact solutions in three dynamical symmetry limits (that is, the anharmonic vibrator $U(5)$, axial rotor $SU(3)$ and γ-unstable rotor $O(6)$ limits), can usually successfully describe the low-lying collective properties of a wide range of nuclei with the inclusion of those in transitional regions. Typically, the $O(6)$ dynamical symmetry of the IBM has been satisfactorily used to describe the low-lying spectra in the region [10, 25]. In addition, Yoshinaga et al. have nicely reproduced the energy spectra of the low-lying states along with intraband and interband E2 transitions for Xe, Ba, Ce, and Nd isotopes within the framework of the pair-truncated shell model, where the collective nucleon pairs with angular momenta zero and two are assumed [14]. Recently, Li et al. [13] have performed constrained self-consistent RMF calculations for triaxial shapes and reproduced the characteristic evolution of excitation spectra and E2 transition probabilities for Ba and Xe nuclei in the mass region $A\geqslant 130$. The TPSM calculations have also been carried out for Nd isotope where the yrast and quasi-γ bands are excellently reproduced [26].

In this work, TRS calculations with the inclusion of non-axial γ deformation will be performed for eight selected even–even $N = 76$ isotones ranging from $^{130}_{54}$Xe to $^{144}_{68}$Er, focusing on the evolution of triaxiality or γ softness with rotation and providing a reasonable prediction especially for ^{142}Dy and ^{144}Er nuclei where data are presently scarce. Similarly, we have previously investigated the evolution of octupole-softness in rotating ^{106,108}Te and neutron-deficient U isotopes [27, 28]. This paper is organized as follows. In Section 2, we give a brief introduction of the TRS method. In Section 3, the calculated results are presented and discussed, where comparison is made with other predictions and experimental data. Finally, a brief summary is given in Section 4.

2 Total Routhian surface method

The TRS calculation applied here is based on the pairing-deformation self-consistent cranked shell model (CSM) [29, 30]. Such an approach usually accounts well for the overall systematics of high-spin phenomena in rapidly rotating medium and heavy mass nuclei. The total Routhian, which is called "Routhian" rather than "energy" in a rotating frame of reference, is the sum of the energy of the non-rotating state, $E^{\omega=0}(Z,N,\hat{\beta})$, and the contribution, $\langle\Psi^{\omega}\,|\,\hat{H}^{\omega}\,|\Psi^{\omega}\rangle$- $\langle\Psi^{\omega}\,|\,\hat{H}^{\omega}\,|\Psi^{\omega}\rangle^{\omega=0}$, due to cranking.

The energy $E^{\omega=0}(Z,N,\hat{\beta})$ consists of a macroscopic part $E_{\rm macr}(Z,N,\hat{\beta})$, being a smooth function of Z, N and deformation, and a fluctuating microscopic part $E_{\rm micr}(Z,N,\hat{\beta})$, which is based on some phenomenological single-particle potential. The macroscopic term is obtained from the sharp-surface standard liquid-drop formula with the parameters used by Myers and Swiatecki [31]. The microscopic correction part, which arises because of the non-uniform distribution of single-particle levels in the nucleus, mainly contains a shell correction $\delta E_{\rm shell}(Z,N,\hat{\beta})$ and a pairing correction $\delta E_{\rm pair}(Z,N,\hat{\beta})$ which are calculated using the Strutinsky method [32] and Lipkin-Nogami (LN) method [33], respectively. These two contributions need to be evaluated from a set of single-particle levels. Here, such single-particle energies are obtained from a deformed Woods–Saxon (WS) potential [34] generated numerically at a deformation specified in terms of the multipole expansion of spherical harmonics $Y_{\lambda\mu}(\theta,\phi)$. In general, a limiting value of $\lambda<A^{1/3}$ can be obtained by a crude estimate [2]. During the diagonalization process of the WS hamiltonian, the eigenfunctions of the axially deformed harmonic oscillator in the cylindrical coordinate system with the principal quantum number $N\leqslant 12$ and 14 have been used as a basis for protons and neutrons, respectively. Strutinsky smoothing is performed with a sixth-order Laguerre polynomial and a smoothing range $\gamma = 1.20\hbar\omega_0$, where $\hbar\omega_0 = 41/A^{1/3}$ MeV. The LN method avoids the spurious pairing phase transition encountered in the simpler BCS calculation. In the pairing windows, dozens of single-particle levels, the respective states (e.g. half of the particle number Z or N) just below and above the Fermi energy, are included empirically for both protons and neutrons. Moreover, not only monopole but also doubly stretched quadrupole pairings are considered. The monopole pairing strength, G, is determined by the average gap method [35] and the quadrupole pairing strengths are obtained by restoring the Galilean invariance broken by the seniority pairing force [36].

Cranking indicates that the nuclear system is constrained to rotate around a fixed axis (e.g. the x-axis) at a given frequency ω. This is equivalent to minimizing the rotation Hamiltonian H^{ω} instead of the Hamiltonian H with respect to variations of the mean field. For a given rotational frequency and point of deformation lattice, this can be achieved by solving the well known Hartree–Fock–Bogolyubov–Cranking (HFBC) equations using a sufficiently large space of single-particle states [29]. Certainly, pairing correlations are dependent on rotational frequency as well as deformation. While solving the HFBC equations, pairing is treated self-consistently and symmetries of the rotating potential are used to simplify the cranking equations. In the reflection-symmetric case, both signature, r, and intrinsic parity, π are good quantum numbers. Then one can obtain the energy relative

to the non-rotating ($\omega=0$) state, as mentioned above. After the numerically calculated Routhians at fixed ω are interpolated using a cubic spline function between the lattice points, the equilibrium deformation can be determined by minimizing the calculated TRS.

3 Results and discussion

As most of the existing cranking calculations, the rotational axis of a triaxial nucleus presently coincides with one of the principal axes with the largest moment of inertia, leading to the lowest-energy (yrast) states. Under the Lund convention, the Cartesian quadrupole coordinates $X=\beta_2\cos(\gamma+30^\circ)$ and $Y=\beta_2\sin(\gamma+30^\circ)$ were used during the actual calculations. The parameter β_2 specifies the magnitude of the quadrupole deformation, while γ specifies the asymmetry of the shape here. The γ parameter covers the range $-120^\circ\leqslant\gamma\leqslant60^\circ$. The three sectors defined by $-120^\circ<\gamma<-60^\circ$, $-60^\circ<\gamma<0^\circ$ and $0^\circ<\gamma<60^\circ$ are equivalent at the ground state, describing the same triaxial shapes, but respectively represent rotation about the long, medium and short axes at nonzero cranking frequency. The four limiting cases, $\gamma=-120^\circ$, 60°, 0° and 60°, correspond to the possible rotations of axially symmetric shapes with various orientations of the nuclear axes with respect to the rotation axis. For instance, for $\gamma=-120^\circ$ (prolate shape) the nucleus rotates around the prolate symmetry axis and for $\gamma=60^\circ$ (oblate shape) it rotates around the oblate symmetry axis; for $\gamma=0^\circ$ (prolate shape) and for $\gamma=-60^\circ$ (oblate shape) the nucleus has a collective rotation around an axis perpendicular to the symmetry axis.

The ground-state deformations β_2, β_4 and γ of the TRS calculations are presented in Table 1 for even–even $N=76$ isotones ranging from ^{130}Xe to ^{144}Er, together with the results based on the fold-Yukawa (FY) single-particle potential and the finite-range droplet model (FRDM) and the partial experimental values obtained from reduced transition probabilities B(E2) [41] for comparison. In addition, the low-lying $E(2_1^+)$, $E(4_1^+)$, $E(2_\gamma^+)$ states and related quantities $R_{4/2}$ ($\equiv E(4_1^+)/E(2_1^+)$, $R_{2/2}$ ($\equiv E(2_\gamma^+)/E(2_1^+)$, are also shown in the table, which usually can provide a test of the axial or non-axial assumption of a nucleus. For instance, the energy ratio $R_{4/2}$ is 3.33 for an axially symmetric rotor and 2.0 for an harmonic vibrator; according to the RTRM [40], the γ parameter describing shape deviations from axial symmetry can be estimated from the energy ratio $R_{2/2}$,

$$R_{2/2}=\left[1+\sqrt{1-\frac{8}{9}\sin^2(3\gamma)}\right]\Big/\left[1-\sqrt{1-\frac{8}{9}\sin^2(3\gamma)}\right],$$

and the deduced γ values are tabled as well. One can see that the energies of the $E(2_1^+)$, $E(4_1^+)$, $E(2_\gamma^+)$ states decrease with the proton number far away from the $Z=50$ closed shell. As expected, the proton mid-shell nucleus $^{142}_{66}$Dy$_{76}$ has the lowest $E(2_1^+)$ state. Our calculated deformation β_2 shows an increasing trend with the proton number far away from the $Z=50$ closed shell and reaches the largest value at $^{142}_{66}$Dy$_{76}$, in good agreement with the above facts. Moreover, our results are closer to experimental data than those of the FY+FRDM calculations. Despite there being a slight discrepancy between the present TRS and other calculations, the general trends are consistent, such as the signs of β_4 and the relatively large γ values.

In a rapidly rotating nucleus, the Coriolis and centrifugal interactions may be strong enough to modify the nucleonic motion and to destroy the superfluid (pairing) correlations and nuclear shape (mean field). Fig. 1 shows the equilibrium deformation parameters β_2 and γ obtained from the calculated TRS minima for frequencies ranging from $\hbar\omega$=0.0 to 0.5 MeV (the corresponding spin maximum of these even–even isotones can be extended

Table 1. The low-lying $E(2_1^+)$, $E(4_1^+)$, $E(2_\gamma^+)$ states [15–21, 37, 38] and related quantities $R_{4/2}$, $R_{2/2}$. The equilibrium deformation parameters β_2, β_4 and γ obtained from the calculated TRS minima at zero frequency for even–even $N=76$ isotones ranging from ^{130}Xe to ^{144}Er, compared with the FY+FRDM (FF) [7, 39] and the RTRM [40] calculations and partial experimental values (Exp.) obtained from reduced transition probabilities B(E2) [41].

nuclei	$E(2_1^+)$	$E(4_1^+)$	$R_{4/2}$	$E(2_\gamma^+)$	$R_{2/2}$	β_2			β_4		$\gamma^{\rm b}/(^\circ)$		
	/keV	/keV		/keV		TRS	FF	Exp.[a]	TRS	FF	TRS	FF	RTRM
$^{130}_{54}$Xe$_{76}$	536.1	1204.6	2.25	1122.1	2.09	0.14	−0.11	0.17	0.00	−0.03	22	30	28
$^{132}_{56}$Ba$_{76}$	464.5	1127.6	2.43	1031.7	2.22	0.16	0.14	0.19	−0.01	−0.01	−100(20)	20	26
$^{134}_{58}$Ce$_{76}$	409.2	1048.7	2.56	965.7	2.36	0.18	0.16	0.20	−0.02	−0.02	23	23	25
$^{136}_{60}$Nd$_{76}$	373.7	976.4	2.61	862.4	2.31	0.19	0.17	—	−0.02	−0.03	25	25	26
$^{138}_{62}$Sm$_{76}$	346.8	891.6	2.57	745.8	2.15	0.21	0.19	0.21	−0.03	−0.04	−94(26)	23	27
$^{140}_{64}$Gd$_{76}$	328.6	836.2	2.54	713.3	2.17	0.22	0.21	—	−0.03	−0.04	−94(26)	20	27
$^{142}_{66}$Dy$_{76}$	315.9	798.9	2.53	—	—	0.23	0.22	—	−0.03	−0.05	−97(23)	20	—
$^{144}_{68}$Er$_{76}$	330.0	—	—	—	—	0.22	0.22	—	−0.04	−0.07	18	—	—

a The uncertainties are less than 0.01 except for $^{138}_{62}$Sm$_{76}$ (< 0.02), see Ref. [41] for details.

b The negative γ values of −100, −94 and −97 are respectively equivalent to the positive 20, 26 and 23 at ground states, representing rotation about different axes, see text for explanation.

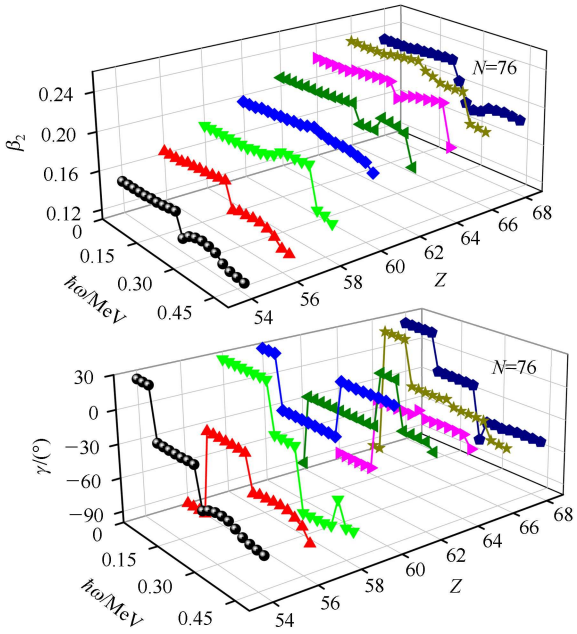

Fig. 1. (color online) Calculated deformation parameters β_2 (top) and γ (bottom) of yrast states for even–even $N=76$ isotones ranging from $^{130}_{54}$Xe to $^{144}_{68}$Er as a function of the rotational frequency $\hbar\omega$.

up to about 17–27 $\hbar$). It can be seen that the β_2 deformations in these nuclei stay almost constant as a function of rotational frequency at first. After certain (one or more) critical frequencies $\hbar\omega$, the β_2 deformations suddenly change (generally decrease) due to the possible rotation-alignment of $1h_{11/2}$ proton or neutron pair. The change of γ value, as discussed above, can provide the evolution information for the triaxial shape and rotational axis. In Fig. 1, for example, one can clearly see that $^{130}_{54}$Xe$_{76}$, $^{134}_{58}$Ce$_{76}$ and $^{144}_{68}$Er$_{76}$ exhibit the evolution of the rotational axes from short-axis (with $0^\circ<\gamma<60^\circ$) to medium-axis (with $-60^\circ<\gamma<0^\circ$) to short-axis (with $-120^\circ<\gamma<-60^\circ$) with increasing frequency.

To obtain a better understanding of the shape evolution of these $N=76$ isotones, we display the calculated aligned angular momentum in Fig. 2, together with proton and neutron components. Obviously, the first substantial increases of the total aligned angular momentum I_x in ^{130}Xe, ^{132}Ba and ^{134}Ce can be attributed to the neutron contribution I_{xn} (the rotation-alignment of a pair of $1h_{11/2}$ neutrons is possible due to the large gain about 10 $\hbar$) and it seems that the rotation-alignment of the second pair of neutrons occurs at higher frequency. Similarly, the first substantial increases of I_x should be caused by the $1h_{11/2}$ proton rotation-alignment in nuclei

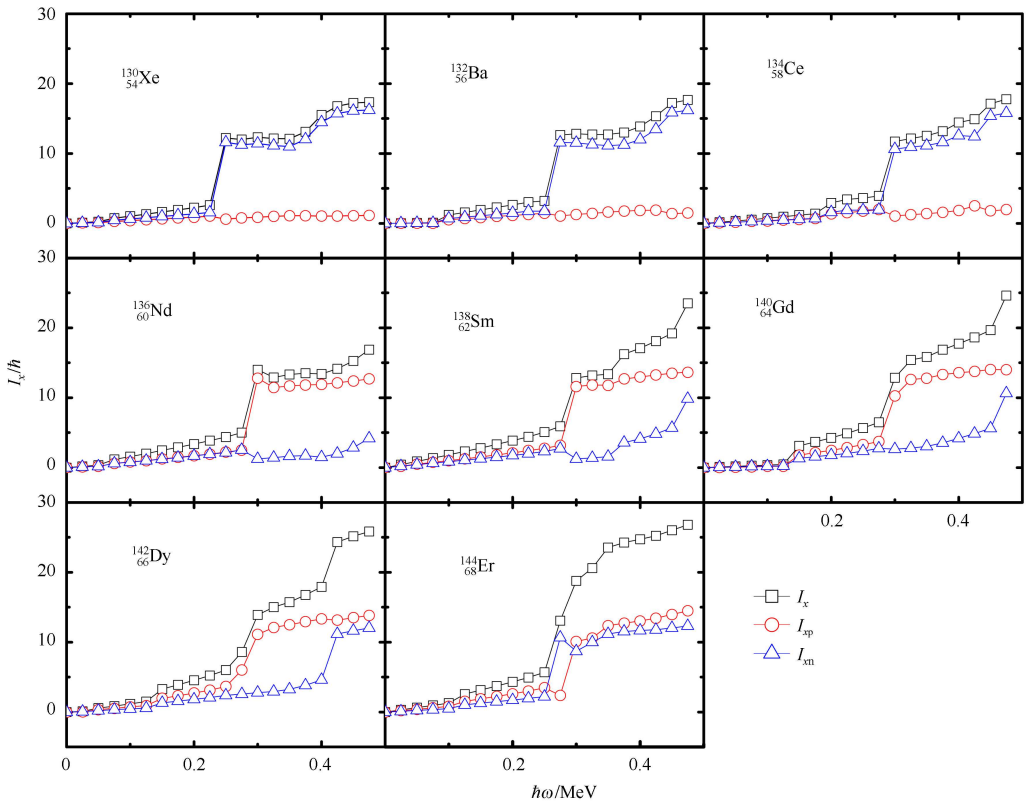

Fig. 2. (color online) Calculated aligned angular momentum against rotational frequency $\hbar\omega$ for even–even $N=76$ isotones ranging from $^{130}_{54}$Xe to $^{144}_{68}$Er. Proton and neutron components are shown simultaneously.

from $^{136}_{60}$Nd$_{76}$ to $^{142}_{66}$Dy$_{76}$, while the second ones by the $1h_{11/2}$ neutron rotation-alignment. These properties are partly supported by the available experimental data [16–21, 37, 38]. In addition, as described in ^{252,254}No [42] and ^{256}Rf [43], it is interesting to find that the alignments of proton and neutron pairs are strongly competitive and take place almost simultaneously in $^{144}_{68}$Er$_{76}$ where only one excited state is observed nowadays [15].

Nuclei in the transitional regions have relatively complicated level structures and soft shapes which may be strongly affected by the mean-field and pairing potential parameters. Therefore, theoretical results usually depend on model parameters to a large extent. However, the rigidity or softness of the nucleus, which is impossible to be seen only from the calculated equilibrium deformations, is almost model-independent and can be evaluated in terms of the corresponding deformation energy curves. As shown in Figs. 3 and 4, we visually show the total Routhian curves along the minimum valley of the TRS in both β_2 and γ directions. To investigate the softness evolution of each nucleus with rotation, four typical rotational frequencies ω = 0.00, 0.15, 0.30 and 0.45 MeV/$\hbar$ are selected. One can see the rotational effect on the quadrupole deformation β_2 is small at low frequency, as shown in Fig. 3, implying that the shape is basically rigid against β_2 variation at the moment, but obvious at higher frequency where the curve is relatively flat, especially in ^{134}Ce and ^{138}Sm, indicating a large softness. Fig. 4 shows that the energy curves as a function of γ deformation are strongly affected by cranking. The evolution of the ω-dependent softness and depth of the local minimum or global minimum is clearly seen as well. The ^{130}Xe, ^{132}Ba and ^{144}Er nuclei have very shallow prolate-triaxial minima at the ground states but deep oblate-triaxial minima at high-spin states. The deeper triaxial minima at the ground states (more than 0.5 MeV) appear in ^{138}Sm and ^{140}Gd, as shown in Table 1, which indeed have lower $E(2^+_\gamma)$ states. Experimentally, the prolate-oblate shape coexistence has been observed in ^{134}Nd [44]. Similarly, it is possible to identify such phenomenon in some $N=76$ isotones, such as ^{134}Ce, ^{136}Nd and ^{142}Dy in which the prolate and oblate triaxial minima with similar energies are found from Fig. 4.

The energy staggering $S(I)$ of the odd- and even-spin levels of a γ band, where $S(I)=\{E(I^+_\gamma)+E[(I-2)^+_\gamma]-2E[(I-1)^+_\gamma]\}/E(2^+_1)$, can usually be viewed as an impor-

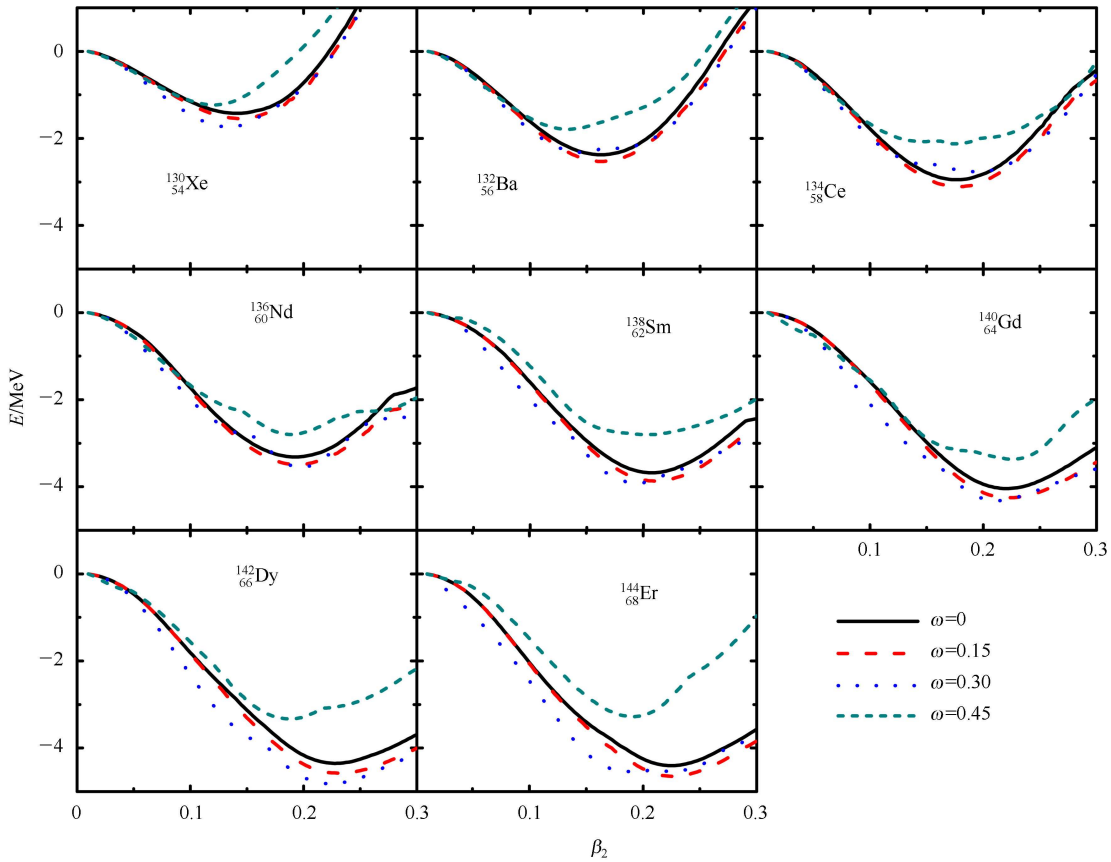

Fig. 3. (color online) Total deformation Routhian curves against β_2 for even–even $N=76$ isotones ranging from ^{130}Xe to ^{144}Er at several selected rotational frequencies ω=0.00 (solid lines), 0.15 (dashed lines), 0.30 (dotted lines) and 0.45 (dashed-dotted lines) MeV/$\hbar$. The energy has been minimized with respect to γ and β_4 at each β_2 point.

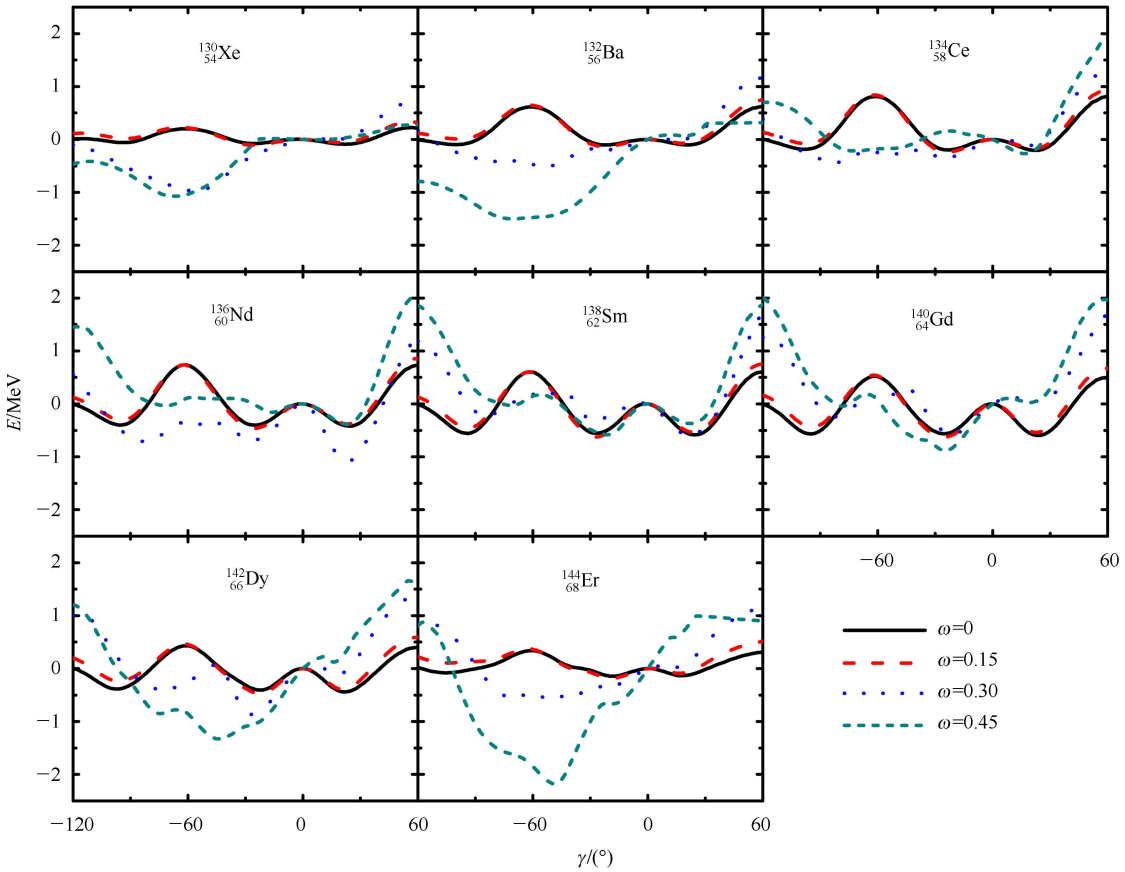

Fig. 4. (color online) Similar to Fig. 3, but with total deformation Routhian curves against γ deformation.

tant structural indicator to distinguish triaxial and γ-soft properties [24, 45]. For a rigid triaxial potential, $S(I)$ will exhibit an oscillating behavior that takes on positive and negative values for even and odd spins, respectively. In both the vibrator and γ-soft limits, an opposite phase appears in $S(I)$, namely positive for odd spin and negative for even spin. Moreover, the overall magnitude of $S(I)$ is larger in the γ-soft limit and increases gradually with spin compared with the vibrator predictions that are smaller in magnitude and constant. For an axially symmetric deformed rotor, the $S(I)$ values are positive, small, and constant as a function of spin [45]. Experimental staggering $S(I)$ for these available $N=76$ isotones are shown in Fig. 5 in comparison with those for a rigid triaxial nucleus ^{76}Ge [46] and an axially symmetric nucleus ^{162}Er [45]. It is unambiguous that the sign of $S(4)$ is negative for all of these nuclei, indicating the vibrator or γ-soft properties. The magnitude of $S(4)$ is smallest for ^{138}Sm and largest for ^{130}Xe. The oscillatory pattern of $S(I)$ observed in ^{132}Ba, ^{134}Ce and ^{140}Gd and at least $S(4)$ and $S(5)$ in ^{130}Xe and ^{136}Nd, opposite to that in ^{76}Ge, agrees with the γ-soft potential predictions. The overall magnitude of the observed staggering clearly displays an increasing trend with spin I and the most obvious example is that in ^{132}Ba. These properties are basically consistent with the ω-dependent energy curves, as shown in Fig. 4. The situation in ^{142}Dy and ^{144}Er cannot be shown due to the scarce data at

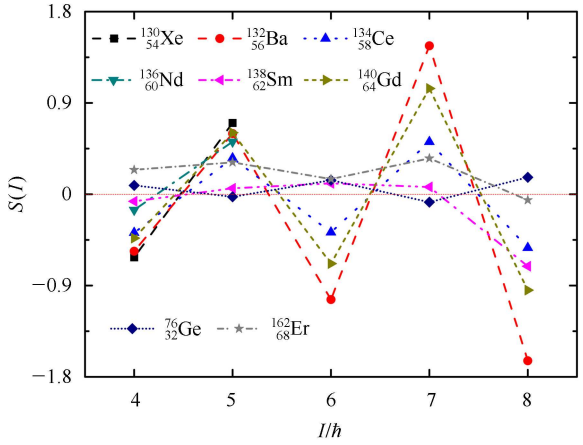

Fig. 5. (color online) Odd–even energy staggering $S(I)$ for even–even $N=76$ isotones ranging from ^{130}Xe to ^{140}Gd [15–21], together with the typical γ-rigid nucleus ^{76}Ge [46] and axially-symmetric nucleus ^{162}Er [45] for comparison.

present. It is worth noting that the energy staggering $S(I)$ in ^{138}Sm shows an anomalous behavior if the γ levels suggested in Ref. [15] are accepted, similar to that in ^{138}Nd [47] where the $S(6)$ value is also positive. It is somewhat necessary to further study such anomalous behavior and of interest to further identify the high-spin levels of the γ band, especially for ^{142}Dy and ^{144}Er in experiments.

4 Summary

In summary, the TRS calculations in the (β_2, γ, β_4) deformation space have been carried out for eight even–even $N=76$ isotones ranging from $^{130}_{54}$Xe to $^{144}_{68}$Er, paying attention to the evolution of the γ-softness and triaxiality with rotation. The calculated equilibrium deformations are compared with previously published results and experiments, which indicates that our results are to some extent closer to the experimental values. The somewhat large uncertainty of the equilibrium deformations in soft nuclei may, to a large extent, be attributed to the difference of model parameters. The shape evolution and nuclear softness in the β_2 and γ directions are evaluated. It is found that the neutron rotation-alignment is preferred in the lighter $N=76$ isotones, while for the heavier ones the proton alignment is favored and their competition is particularly strong for $^{144}_{68}$Er in which data is to date scarce. The energy staggering $S(I)$ of available γ bands are in basic agreement with the analytic results of corresponding deformation-energy curves. In addition, similar to most models, the present method can only describe nuclear structure to some extent. For the transitional soft nuclei, it should be important to consider some other effects, e.g., the rotation-vibration coupling.

References

1 LU B N, ZHAO J, ZHAO E G, ZHOU S G. Phys. Rev. C, 2014, **89**: 014323
2 Greiner W, Maruhn J A. Nuclear Models. Springer-Verlag, 1996, 108–115
3 Ødegård S W, Hagemann G B, Jensen D R et al. Phys. Rev. Lett., 2001, **86**: 5866–5869
4 Bengtsson R, Frisk H, May F R et al. Nucl. Phys. A, 1984, **415**: 189–214
5 Starosta K, Koike T, Chiara C J et al. Phys. Rev. Lett., 2001, **86**: 971–974
6 SHEN S F, ZHENG S J, XU F R et al. Phys. Rev. C, 2011, **84**: 044315
7 Möller P, Bengtsson R, Carlsson B G et al. At. DATA Nucl. Data Tables, 2008, **94**: 758–782
8 Davydov A S, Filippov G F. Nucl. Phys., 1958, **8**: 237–249
9 Bhat G H, Dar W A, Sheikh J A et al. Phys. Rev. C, 2014, **89**: 014328
10 Casten R F, von Brentano P. Phys. Lett. B, 1985, **152**: 22–28
11 Takahashi T, Yoshinaga N, Higashiyama K. Phys. Rev. C, 2005, **71**: 014305
12 PAN X W, PING J L, FENG D H et al. Phys. Rev. C, 1996, **53**: 715–729
13 LI Z P, Nikšić T, Vretenar D et al. Phys. Rew. C, 2010, **81**: 034316
14 Yoshinaga N, Higashiyama K. Phys. Rev. C, 2004, **69**: 054309
15 http://www.nndc.bnl.gov/
16 Goettig L, Droste Ch, Dygo A et al. Nucl. Phys. A, 1981, **357**: 109–125
17 Juutinen S, Törmänen S, Ahonen P et al. Phys. Rev. C, 1995, **52**: 2946–2954
18 Gade A, Wiedenhöver I, Luig M et al. Nucl. Phys. A, 2000, **673**: 45–63
19 Petrache C M, Bazzacco D, Lunardi S et al. Phys. Lett. B, 1996, **373**: 275–281
20 Paul E S, Beausang C W, Clark R M et al. J. Phys. G, 1994, **20**: 1405–1421
21 Paul E S, Ahn K, Fossan D B et al. Phys. Rev. C, 1989, **39**: 153–157
22 Kern B D, Mlekodaj R L, Leander G A et al. Phys. Rev. C, 1987, **36**: 1514–1521
23 Wilets L, Jean M. Phys. Rev., 1956, **102**: 788–796
24 Zamfir N V, Casten R F. Phys. Lett. B, 1991, **260**: 265–270
25 Saito T R, Satio N, Starosta K et al. Phys. Lett. B, 2008, **669**: 19–23
26 LI H J, XIAO Z G, ZHU S J et al. Phys. Rev. C, 2013, **87**: 057303
27 WANG H L, LIU H L, XU F R et al. Prog. Theo. Phys., 2012, **128**: 363–371
28 WANG H L, LIU H L, XU F R. Phys. Scr., 2012, **86**: 035201
29 Satuła W, Wyss R, Magierski P. Nucl. Phys. A, 1994, **578**: 45–61
30 XU F R, Satuła W, Wyss R. Nucl. Phys. A, 2000, **669**: 119–134
31 Myers W D, Swiatecki W J. Nucl. Phys., 1966, **81**: 1–60
32 Strutinsky V M. Nucl. Phys. A, 1967, **95**: 420–442
33 Pradhan H C, Nogami Y, Law J. Nucl. Phys. A, 1973, **201**: 357–368
34 Ćwiok S, Dudek J, Nazarewicz W et al. Comp. Phys. Comm., 1987, **46**: 379–399
35 Möller P, Nix J R. Nucl. Phys. A, 1992, **536**: 20–60
36 Sakamoto H, Kishimoto T. Phys. Lett. B, 1990, **245**: 321–324
37 Goettig L, Gelletly W, Lister C J et al. Nucl. Phys. A, 1987, **475**: 569–578
38 Seweryniak D, Blank B, Carpenter M P et al. Phys. Rev. Lett., 2007, **99**: 082502
39 Möller P, Nix J R, Myers W D et al. At. Data Nucl. Data Tables, 1995, **59**: 185–381
40 YAN J, Vogel O, Brentano P von et al. Phys. Rev. C,1993, **48**: 1046–1049
41 Raman S, Nestor Jr C W, Tikkanen P. Atomic Data and Nuclear Data Tables, 2001, **78**: 1–128
42 Al-Khudair F, LONG G L, SUN Y. Phys. Rev. C, 2009, **79**: 034320
43 WANG H L, CHAI Q Z, JIANG J G et al. Chin. Phys. C, 2014, **38**: 074101
44 Petrache C M, SUN Y, Bazzacco D et al. Nucl. Phys. A, 1997, **617**: 249–264
45 McCutchan E A, Bonatsos D, Zamfir N V et al. Phys. Rev. C, 2007, **76**: 024306
46 Toh Y, Chiara C J, McCutchan E A et al. Phys. Rev. C, 2013, **87**: 041304(R)
47 CHAI Q Z, WANG H L, YANG Q et al. Chin. Phys. C, 2015, **39**: 024101